

SURFACE MODIFICATION OF AN $\text{Al}_2\text{O}_3/\text{SiO}_2$ BASED CERAMIC TREATED WITH CO_2 , Nd:YAG, EXCIMER AND HIGH POWER DIODE LASERS FOR ALTERED WETTABILITY CHARACTERISTICS

J. Lawrence *, L. Li * and J.T. Spencer **

* Department of Mechanical Engineering, UMIST, Manchester, M60 1QD, UK.

** Research & Technology, B709, BNFL, Springfields Works, Preston, PR4 0XJ, UK.

ABSTRACT

Interaction of CO_2 , Nd:YAG, excimer and high power diode laser (HPDL) radiation with the surface of an $\text{Al}_2\text{O}_3/\text{SiO}_2$ based ceramic was found to affect significant changes in the wettability characteristics of the material. It was observed that interaction with CO_2 , Nd:YAG and HPDL radiation reduced the enamel contact angle from 118° to 31° , 34° and 33° respectively. In contrast, interaction with excimer laser radiation resulted an increase in the contact angle to 121° . Such changes were identified as being due to: (i) the melting and partial vitrification of the $\text{Al}_2\text{O}_3/\text{SiO}_2$ based ceramic surface as a result of interaction with CO_2 , Nd:YAG HPDL radiation. (ii) the surface roughness of the $\text{Al}_2\text{O}_3/\text{SiO}_2$ based ceramic increasing after interaction with excimer laser radiation. (iii) the relative surface oxygen content of the $\text{Al}_2\text{O}_3/\text{SiO}_2$ based ceramic increasing after interaction with CO_2 , Nd:YAG and HPDL radiation. The work has shown that the wettability characteristics of the $\text{Al}_2\text{O}_3/\text{SiO}_2$ based ceramic could be controlled and/or modified with laser surface treatment. Moreover, it was found that changes in the wettability characteristics of the $\text{Al}_2\text{O}_3/\text{SiO}_2$ based ceramic are related to the effects of laser wavelength, that is whether the wavelength of the laser radiation has the propensity to cause surface melting.

1. INTRODUCTION

Comparisons of the differences in the beam interaction characteristics with various materials of the predominant materials processing lasers, the CO_2 , the Nd:YAG and the excimer laser, are not very well documented. Likewise, such practical comparisons between these traditional materials processing lasers and the more contemporary high power diode laser (HPDL) are even fewer in number. This paper reports on work conducted to determine the differences in the beam interaction characteristics of an $\text{Al}_2\text{O}_3/\text{SiO}_2$ based ceramic material and a commercially available vitreous enamel with a 1 kW CO_2 laser, a 400 W Nd:YAG laser, a KrF excimer laser and a 60 W-cw HPDL, with particular emphasis on the laser affected modification of the wettability characteristics. The $\text{Al}_2\text{O}_3/\text{SiO}_2$ based ceramic used in this present study is a newly developed ceramic tile grout material (an amalgamated oxide compound grout (AOCG)), which in practice is sealed by firing the enamel frit onto it using a HPDL, thus creating an impervious surface glaze [1-3].

Both scientists and engineers alike have a great interest in understanding the interfacial phenomena between vitreous enamels and ceramic materials, since in many practical applications where vitreous enamels are fired onto ceramic substrates, the performance of the article is directly linked to the nature of the enamel-ceramic interface. At present, very little work has been published with regard to the use of lasers for altering the surface properties of materials in order to improve their wettability characteristics. Notwithstanding this, it is recognised within the currently published work that laser irradiation of material surfaces can effect its wettability characteristics. Previously Zhou et al [4, 5] have carried out work on laser coating of aluminium

alloys with ceramic materials (SiO_2 , Al_2O_3 , etc.), reporting on the well documented fact that generated oxide layers often promote metal/oxide wetting. Bahners et al [6, 7], have observed and comprehensively detailed the changes in technical properties of various textile fibres, including adhesion and wetting properties, with a view to developing an alternative to the conventional methods of chemical agents addition or wet-chemical pre-processing. Also, Heitz et al [8] and Olfert et al [9] have found that excimer laser treatment of metals results in improved coating adhesion. The improvements in adhesion were ascribed to the fact that the excimer laser treatment resulted in a smoother surface and as such enhanced the action of wetting. However, the reasons for these changes with regard to changes in the material's surface morphology, surface composition and surface energy are not reported.

This paper reports specifically on the interaction characteristics of the beams of all four lasers with the AOCG and the enamel in terms of resultant changes in the wettability characteristics. These incorporate chiefly: contact angle variations, the differences in morphological features, the surface composition, the microstructural changes and the surface energy changes.

2. EXPERIMENTAL PROCEDURE

2.1 Laser Processing Procedures

The formulation procedure of the AOCG is detailed elsewhere [1-3]. Figure 1 schematically illustrates the general laser processing experimental arrangement, where the defocused beams of the lasers were fired back and forth across the surfaces of the AOCG by traversing the samples beneath the laser beam using the x- and y-axis of the CNC gantry table. For means of comparison the laser power densities and traverse speeds used were manipulated such that the energy density incident upon the AOCG surface was around 165 J/cm^2 .

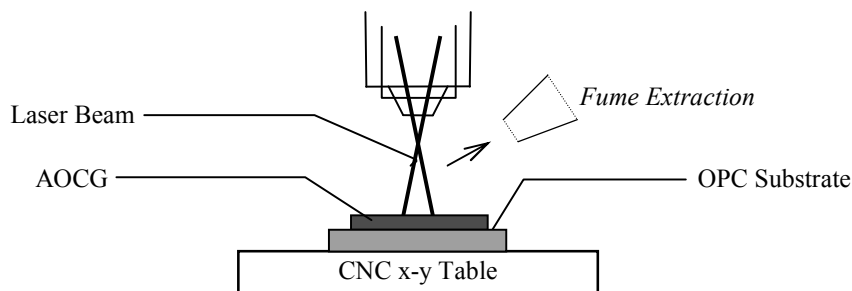


Figure 1. Schematic of the set-up for the CO_2 , Nd:YAG, HPDL and excimer laser interaction experiments with the AOCG.

2.2 Contact Angle and Surface Energy Analysis Procedure

To investigate the effects of laser wavelength on the wetting and surface energy characteristics of the AOCG, two sets of wetting experiments were conducted. The first set of experiments were to simply determine the contact angle between the enamel and the AOCG before and after interaction with the selected industrial lasers. The second set of experiments were control experiments carried out using the sessile drop technique with a variety of test liquids with known surface energy properties in order to quantify any surface energy changes in the AOCG resulting from laser interaction.

The enamel-AOCG wetting experiments were carried out in atmospheric conditions with molten droplets of the enamel (600°C). The temperature of the enamel throughout the experiments was measured using a Cyclops infrared pyrometer. The droplets were released in a controlled manner onto the surface of the AOCG (laser treated and untreated) from the tip of a micropipette, with the resultant volume of the drops being

approximately $15 \times 10^{-3} \text{ cm}^3$. Profile photographs of the sessile enamel drop were obtained for every 60°C fall in temperature of the molten enamel drop, with the contact angle subsequently being measured.

The sessile drop control experiments were carried out using human blood, human blood plasma, glycerol and 4-octanol; liquids with well established total surface energy (γ_2), dispersive (γ_{lv}^d) and polar (γ_{lv}^p) component values [10]. The experiments were conducted in atmospheric conditions at a temperature of 20°C . The droplets were released in a controlled manner onto the surface of the test substrate materials (laser treated and untreated) from the tip of a micropipette, with the resultant volume of the drops being approximately $6 \times 10^{-3} \text{ cm}^3$. Each experiment lasted for three minutes with profile photographs of the sessile drops being obtained every minute. The contact angles were then subsequently measured.

It was observed during the wetting experiments conducted with both the enamel and the control liquids that, throughout the period of the experiments, no discernible change in the magnitude of the contact angle was observed, indicating that thermodynamic equilibrium was established at the solid-liquid interface at the outset of the experiments.

3. EFFECTS OF LASER WAVELENGTH ON CONTACT ANGLE CHARACTERISTICS

Prior to laser treatment of the AOCG surface it was not possible to fire the enamel onto the surface of the AOCG. This was found to be due to the fact that the contact angle between the enamel and the untreated AOCG surface was measured as being 118.22° , consequently preventing the enamel from wetting the AOCG surface. Figure 2 shows the measured contact angles between the enamel and the surface of the AOCG before and after interaction with the selected industrial lasers.

Figure 2 shows clearly that under the experimental laser parameters, interaction with the CO_2 laser, the Nd:YAG laser and the HPDL beams resulted in the contact angle between the enamel and the AOCG reducing from 118.22° to 31.49° , 34.65° and 33.19° respectively. In contrast, interaction of the AOCG with excimer laser radiation affected an increase in the contact angle to 121.63° .

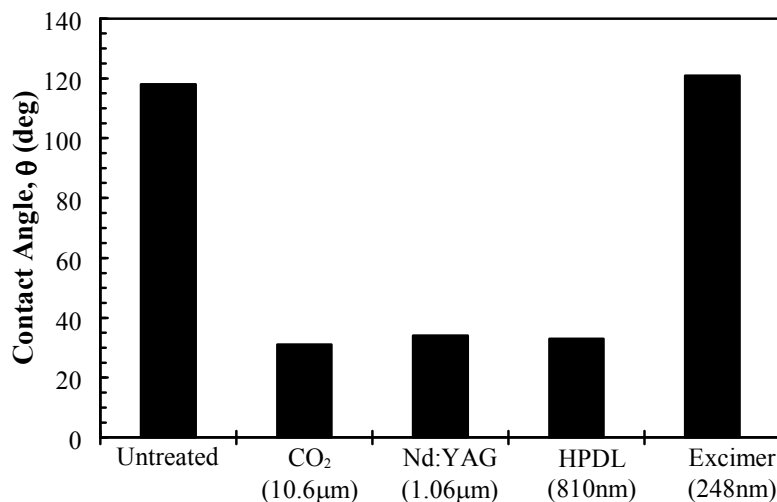


Figure 2. Mean values of contact angles formed between the enamel and the AOCG before and after interaction with the selected lasers.

Similarly, as Table 1 shows, with all the control liquids used the AOCG experienced a significant reduction in contact angle as a result of interaction with the CO_2 laser, the Nd:YAG laser and the HPDL beams, whilst interaction with the excimer laser beam again resulted in an increase in the contact angle.

Table 1. Mean values of contact angles formed between the selected test liquids at 20°C and the AOCG before and after interaction with the selected lasers.

Liquid	Contact Angle, θ (deg)				
	Untreated	CO ₂	Nd:YAG	HPDL	Excimer
Human Blood	60.63	34.49	37.93	36.81	74.34
Human Blood Plasma	63.94	35.45	38.98	37.78	83.69
Glycerol	33.89	26.64	29.22	28.36	56.63
4-Octonol	28.51	24.49	26.64	25.86	43.95

3.1 Variations in Surface Roughness Characteristics

According to Neumann [11, 12], a model similar to that for heterogeneous solid surfaces can be developed in order to account for surface irregularities, being given by a rearrangement Wenzel's equation:

$$\gamma_{sl} = \gamma_{sv} \left(\frac{\gamma_{lv} \cos \theta_w}{r} \right) \quad (1)$$

where, r is the roughness factor defined as the ratio of the real and apparent surface areas, γ_{sv} and γ_{lv} , are the solid and liquid surface energies, γ_{sl} is the solid-liquid interfacial energy and θ_w is the contact angle for the wetting of a rough surface. Equation (1) shows clearly that if the smoothness of the solid surface, r , is large, that is the solid surface is smooth, then γ_{sl} will become small, thus, a reduction in the contact angle will be inherently realised by the liquid since $\gamma_{sv} = \gamma_{lv} \cos \theta + \gamma_{sl}$.

Indeed, as Figure 3 shows, considerable reductions in the surface roughness of the AOCG were observed after interaction with the CO₂ laser, the Nd:YAG laser and the HPDL beams, reducing from an initial Ra value of 25.85 μ m to 5.88 μ m, 6.56 μ m and 6.27 μ m respectively. In contrast, interaction of the AOCG with excimer laser radiation resulted in a roughening of the AOCG surface, causing the surface roughness to increase to an Ra value of 36.22 μ m.

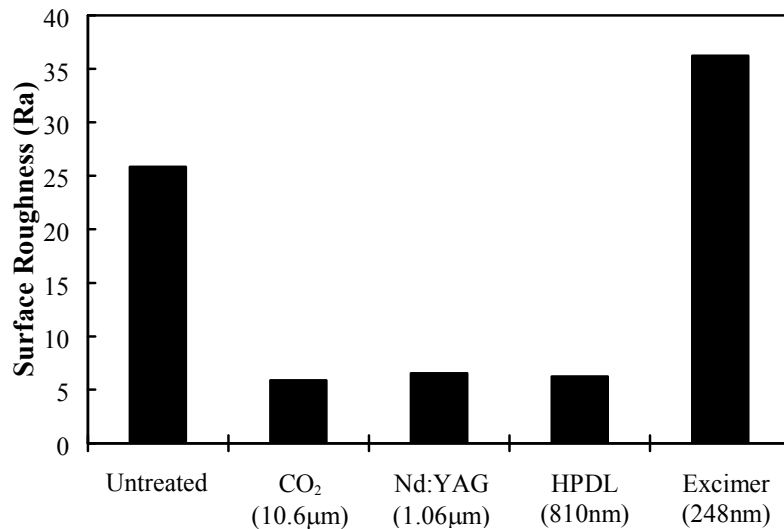


Figure 3. Mean values of surface roughness on the AOCG before and after interaction with the selected lasers.

The smoothing effects of CO₂ laser, Nd:YAG laser and HPDL irradiation on the surface of the AOCG in comparison with the roughening effects of excimer laser irradiation are clearly discernible from Figure 4.

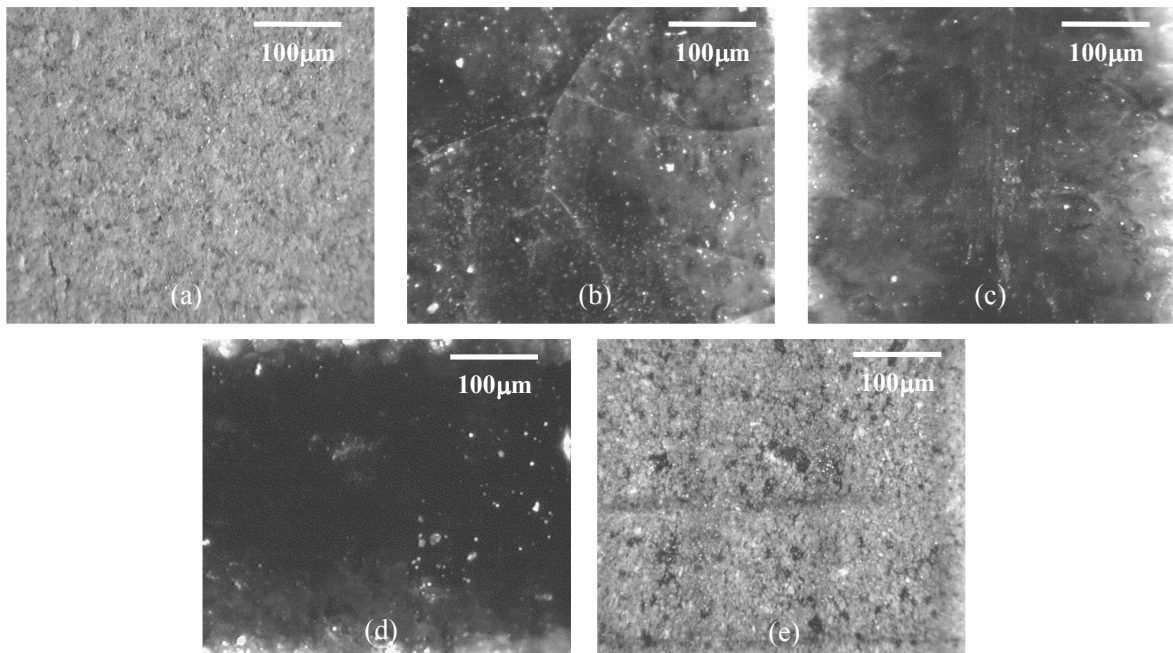


Figure 4. Typical surface images of the AOCG (a) before laser treatment and after laser interaction with (b) CO₂ laser, (c) Nd:YAG laser, (d) HPDL and (e) excimer laser radiation.

3.2 Variations in Surface Oxygen Content

The O₂ content of the AOCG surface is most certainly an influential factor affecting the wetting performance of the AOCG [13 ,14]. Indeed, by mounting cross-sectioned samples of the untreated and laser treated AOCG adjacent to one another, and examining them both simultaneously by means of EDX analysis, it was possible to determine the relative element content of O₂ near to the surface. Probing was conducted at a depth of approximately 1µm below the surface on all the samples.

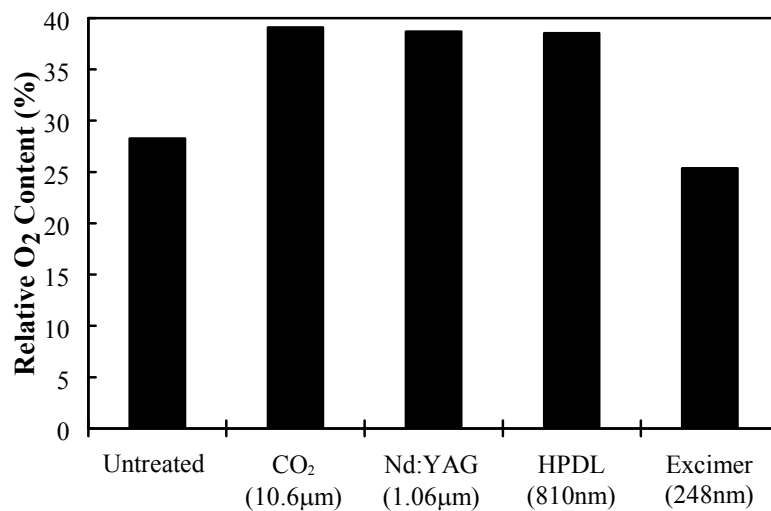


Figure 5. AOCG surface O₂ content before and after interaction with the selected lasers.

Figure 5 shows that differences in the surface O₂ content of the AOCG resulted from interaction with all the selected lasers. As one can see from Figure 5, increases in the surface O₂ content were experienced by the AOCG after interaction with CO₂ laser, the Nd:YAG laser and the HPDL beams, increasing from an initial value of 28.27% to 39.08%, 38.39% and 38.53% respectively. Conversely, interaction of the AOCG with excimer laser radiation resulted in the surface O₂ content of the AOCG decreasing slightly to 25.36%.

4. SURFACE ENERGY AND THE DISPERSIVE/POLAR CHARACTERISTICS

It is possible to estimate reasonably accurately the dispersive component of the AOCG surface energy, γ_{sv}^d , by plotting the graph of $\cos \theta$ against $(\gamma_{lv}^d)^{1/2}/\gamma_{lv}$ in accordance with Equation (2) [15], with the value of γ_{sv}^d being estimated by the gradient ($=2(\gamma_{sv}^d)^{1/2}$) of the line which connects the origin ($\cos \theta = -1$) with the intercept point of the straight line ($\cos \theta$ against $(\gamma_{lv}^d)^{1/2}/\gamma_{lv}$) correlating the data point with the abscissa at $\cos \theta = 1$.

$$\cos \theta = \frac{2(\gamma_{sv}^d \gamma_{lv}^d)^{1/2} + 2(\gamma_{sv}^p \gamma_{lv}^p)^{1/2}}{\gamma_{lv}} - 1 \quad (2)$$

Figure 6 shows the best-fit plot of $\cos \theta$ against $(\gamma_{lv}^d)^{1/2}/\gamma_{lv}$ for the untreated and laser treated AOCG-experimental control liquids system.

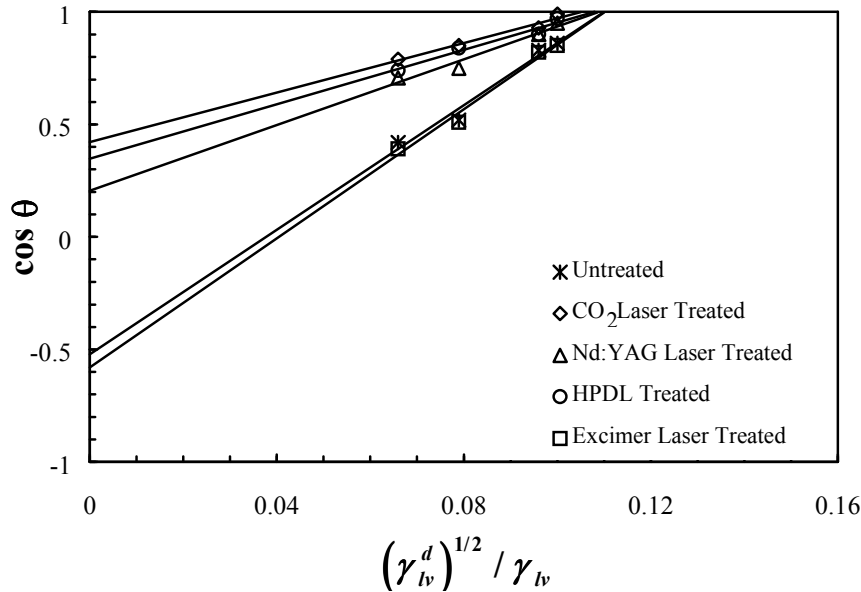


Figure 6. Plot of $\cos \theta$ against $(\gamma_{lv}^d)^{1/2}/\gamma_{lv}$ for the AOCG in contact with the wetting test control liquids, before and after laser treatment.

A comparison of the ordinate intercept points of the untreated and laser treated AOCG-liquid systems, shown in Figure 6, shows clearly that for the untreated and excimer laser treated AOCG-liquid systems, the best-fit straight line intercepts the ordinate relatively close to the origin. In contrast, Figure 6 shows that the best-fit straight line for the AOCG-liquid systems of the CO₂, Nd:YAG and HPDL treated samples intercept the ordinate considerably higher above the origin. This is of great importance since interception of the ordinate

close to the origin is characteristic of the dominance of dispersion forces acting at the AOCG-liquid interfaces of the untreated and excimer laser treated samples, resulting in poor adhesion [15, 16]. While an interception of the ordinate well above the origin is indicative of the action of polar forces across the interface, in addition to dispersion forces, hence improved wettability and adhesion is promoted [15, 16]. Such conditions are clearly apparent from Table 2. Furthermore, because none of the best-fit straight lines intercept below the origin, then it can be said that the development of an equilibrium film pressure of adsorbed vapour on the AOCG surface (untreated and laser treated) did not occur [15, 16].

It is not possible to determine the value of the polar component of the AOCG surface energy, γ_{sv}^p , directly from Figure 6. This is because the intercept of the straight line ($\cos \theta$ against $(\gamma_{lv}^d)^{1/2}/\gamma_{lv}$) is at $2(\gamma_{sv}^p \gamma_{lv}^p)^{1/2}/\gamma_{lv}$, and thus only refers to individual control liquids and not the control liquid system as a whole. However, it has been established that the entire amount of the surface energies due to dispersion forces either of the solids or the liquids are active in the wettability performance [15, 17]. As such, it is possible to calculate the dispersive component of the work of adhesion, W_{ad}^d , thus [15]

$$W_{ad}^d = 2(\gamma_{sv}^d \gamma_{lv}^d)^{1/2} \quad (3)$$

Both W_{ad} and W_{ad}^d are related by the straight line relationship [15]

$$W_{ad} = aW_{ad}^d + b \quad (4)$$

Thus, from the best-fit straight line plots of W_{ad} against W_{ad}^d for the AOCG when it is both untreated and laser treated it is possible to determine the constants a and b for each separate condition of the AOCG. Since a linear relationship exists between the dispersive and polar components of the control test liquids surface energies, then it is possible to calculate directly γ_{sv}^p for untreated and laser treated AOCG using

$$(\gamma_{sv}^p)^{1/2} (\gamma_{lv}^p)^{1/2} = (a - 1)(\gamma_{sv}^d)^{1/2} (\gamma_{lv}^p)^{1/2} + \frac{b}{2} \quad (5)$$

Table 2. Determined surface energy values for the AOCG before and after laser irradiation.

Surface Energy Component	AOCG Condition				
	Untreated	CO ₂	Nd:YAG	HPDL	Excimer
Dispersive Component, γ_{sv}^d (mJ/m ²)	84.16	90.70	86.61	89.04	76.95
Polar Component, γ_{sv}^p (mJ/m ²)	2.00	36.83	36.16	25.87	0.29
Total, γ_{sv} (mJ/m ²)	86.16	127.53	122.77	114.91	77.24

As one can see from Table 2, CO₂ laser, Nd:YAG laser and HPDL treatment of the surface of the AOCG result in an overall increase in the total surface energy γ_{sv} , whilst significantly increasing also the polar component of the surface energy γ_{sv}^p . Such increases in the surface energy of the AOCG, in particular the increase in γ_{sv}^p , have a positive effect upon the action of wetting and adhesion. Again, these changes in the surface energy of the AOCG after treatment with these lasers is primarily due to the fact that the treatment of the AOCG surface results in the partial vitrification of the surface; a transition that is known to affect an increase in γ_{sv}^p [16], consequently causing a decrease in the contact angle.

5. DISCUSSION OF LASER AFFECTED WETTABILITY CHARACTERISTICS MODIFICATION

The results detailed previously show clearly that interaction of the AOCG with selected industrial lasers has resulted in the contact angle formed between the enamel and the control liquids altering to various degrees depending upon the laser type, or more succinctly, the laser beam wavelength. Typically, interaction of the AOCG with the CO₂ laser, the Nd:YAG laser and the HPDL beams resulted in decrease of similar proportion in the contact angle, whilst interaction of the AOCG with excimer laser radiation resulted in an increase in the contact angle. Such changes in the value of the contact angle are influenced, depending upon the laser used, primarily by:

1. *Surface Melting and Partial Vitrification* - Laser induced melting and vitrification results in the occurrence of two main changes in the surface condition of the AOCG. These are:
 - i. *Surface Smoothing* resulting from the laser melting of the AOCG surface which consequently results in a reduction of the surface roughness, thus directly reducing the contact angle, θ .
 - ii. *Increase in the Polar Component, γ_{sv}^p , of the Surface Energy* resulting from the melting and partial laser vitrification of the glass forming elements within the AOCG composition, thus improving the action of wetting and adhesion by generating a surface with a more amorphous surface microstructure.
2. *Surface Roughening* - An increase in the AOCG surface roughness resulting from laser ablation of the AOCG surface in turn results directly in an increase in the contact angle, θ .
3. *Surface O₂ Content* - An increase in the surface O₂ content of the AOCG resulting from laser treatment is an influential factor in the promotion of the action of wetting, since an increase in surface O₂ content inherently affects a decrease in the contact angle, and vice versa.

It is highly likely that the resultant contact angle between the AOCG-enamel and the AOCG-liquid systems of the CO₂, Nd:YAG and the HPDL treated samples are all similar in value due to the fact that interaction with these lasers caused surface melting (see Figure 4), resulting in a significantly smoother surface. This, combined with the fact that vitrification of the AOCG surface results in an increase in the polar component of the surface energy, γ_{sv}^p , as a result of the surface becoming less crystalline in nature, thus promoting wetting, would influence a reduction in the contact angle. And, since the energy densities used were the same for all of the lasers, one would expect the degree of melting and vitrification to be similar. Indeed, from Table 2 it can be seen that interaction of the AOCG with CO₂, Nd:YAG and the HPDL radiation resulted in similar increases in γ_{sv}^p . However, absorption of CO₂ radiation by the AOCG is higher than that of the Nd:YAG or the HPDL [19], and, since contact angle reduction is a function of surface melting and vitrification [19], then surface melting and vitrification will occur to a greater extent with the CO₂ laser, thus resulting in a marginally greater decrease in the contact angle.

In contrast, as Figure 4(e) shows, interaction of the AOCG with excimer laser radiation did not cause melting of the surface, but instead induced surface ablation which consequently resulted in a slightly rougher surface. Thus an increase in the contact angle was affected. Additionally, Kokai et al [20] have concluded that, with excimer laser parameters which are conducive to the production of plasma, as was the case with the AOCG, then the surface roughness is increased as a result of plasma induced debris redepositing on the surface and excessive thermally induced surface fractures and porosities. Clearly, since plasma generation was observed, then surface roughening after excimer laser irradiation was perhaps to be expected. However, Nicolas et al [21] have reported that irradiating ZrO₂ with excimer laser radiation with energy densities in excess of 2.7 J/cm², resulted in a reduction in surface roughness. Such reductions were attributed to the fact that at these levels of energy density, melting of the ZrO₂ surface occurred.

It is also of great importance to consider the surface O₂ content of the AOCG before and after treatment with the selected lasers. As Figure 5 shows, increases in the surface O₂ content were experienced by the AOCG after interaction with CO₂ laser, the Nd:YAG laser and the HPDL beams, whilst interaction of the AOCG

with excimer laser radiation resulted in the surface O₂ content of the AOCG decreasing slightly. Such a result is in agreement with the findings of a number of workers [22, 23], who have noted that for many ceramic materials, irradiation with an excimer laser beam creates defective energy levels, in particular the formation of O₂ vacancies.

Since roughening of the surface does not necessarily create a surface with a more crystalline structure, then it is reasonable to assume that the increase in the surface roughness after excimer laser irradiation, along with the associated reduction on the surface O₂ content, are the principal reasons for the observed decrease in the contact angle.

6. CONCLUSION

Interaction of CO₂, Nd:YAG, excimer and HPDL radiation with the surface of the AOCG was found to affect significant changes in the wettability characteristics of the material. It was observed that interaction with CO₂, Nd:YAG and HPDL radiation reduced the enamel contact angle from 118° to 31°, 34° and 33° respectively. In contrast, interaction with excimer laser radiation resulted an increase in the contact angle to 121°. Such changes were identified as being primarily due to: (i) the melting and partial vitrification of the AOCG surface as a result of interaction with CO₂, Nd:YAG and HPDL radiation. This in turn generated a smoother surface and increased the polar component of the AOCG surface energy. (ii) the surface roughness of the AOCG increasing after interaction with excimer laser radiation due to ablation of the surface which in turn resulted directly in an increase in the contact angle. (iii) the relative surface oxygen content of the AOCG increasing after interaction with CO₂, Nd:YAG and HPDL radiation due to surface melting. The work has shown that changes in the wettability characteristics of the AOCG are related to the effects of laser wavelength, that is whether or not the wavelength of the laser radiation has a propensity to cause surface melting. Similar effects of laser surface treatment have been observed for other ceramic materials when treated with a HPDL [24].

7. ACKNOWLEDGEMENTS

The authors would like to express their gratitude to the EPSRC: Process Engineering Group (Grant No. GR/K99770), the EPSRC: CDP Group (CASE Award No. 95562556) and BNFL for their financial support. The authors are also grateful to the University of Salford (Thierry Fourier & Jason Anderson) for kindly allowing them to use their excimer laser.

REFERENCES

1. Lawrence, J., Li, L., Spencer, J.T., (1996), "Ceramic Tile Grout Removal and Sealing Using High Power Lasers", *Proceedings of ICALEO'96: Laser Materials Processing*, Detroit, USA, Vol 81A, pp 138-148.
2. Lawrence, J., Li, L., Spencer, J.T., (1998), "A Two-Stage Ceramic Tile Grout Sealing Process Using a High Power Diode Laser, Part I: Grout Development and Materials Characteristics", *Optics & Laser Technology*, Vol 30 (3-4), pp 205-214.
3. Lawrence, J., Li, L., Spencer, J.T., (1998), "A Two-Stage Ceramic Tile Grout Sealing Process Using a High Power Diode Laser, Part II: Mechanical, Chemical and Physical Properties", *Optics & Laser Technology*, Vol 30 (3-4), pp 215-223.
4. Zhou, X.B., De Hosson, J.Th.M., (1993), "Microstructure and Interfaces of a Reaction Coating on Aluminium Alloys by Laser Processing", *Journal de Physique IV*, Vol 3, pp 1007-1011.
5. Zhou, X.B., De Hosson, J.Th.M., (1994), "Metal-Ceramic Interfaces in Laser Coated Aluminium Alloys", *Acta Metallurgica et Materialia*, Vol 42 (4), pp 1155-1162.

6. Bahners, T. Kesting W., Schollmeyer, E., (1993), "Designing Surface Properties of Textile Fibres by UV Laser Irradiation", *Applied Surface Science*, Vol 69 (1-4), pp 12-15.
7. Bahners, T., (1993), "Laser Irradiation of Synthetic Fibres as a New Process for the Surface Modification of Textiles- A Review," *Optics & Quantum Electronics*, Vol 27, pp 1337-1348.
8. Heitz J, Arenholz E, Kefer T, Bäuerle D, Hibst H and Hagemeyer A 1992 *App. Phys. A* **55** 391-92
9. Olfert M, Duley W and North T 1996
10. Gutowski, V.W., Russell, L., Cerra, A., (1992), "Adhesion of Silicone Sealants to Organic-Coated Aluminium" in *Science and Technology of Building Seals, Sealants, Glazing and Waterproofing*, (Ed. J.M. Klosowski), Philadelphia: ASTM, pp 144-159.
11. Neumann, A.W., Good, R.J., (1972), "Thermodynamics of Contact Angles: Heterogeneous Solid Surfaces", *Journal of Colloid and Interface Science*, Vol 38 (2), pp 341-351.
12. Neumann, A.W. (1978), "Contact Angles", in *Wetting Spreading and Adhesion*, (Ed. J.F. Padday), London: Academic Press, pp 3-35.
13. Ueki, M., Naka, M., Okamoto, I., (1986), "Wettability of Some Metals Against Zirconia Coatings", *Journal of Materials Science Letters*, Vol 5, pp 1261-1262.
14. Li, J.G., (1993), "Microscopic Approach of Adhesion and Wetting of Liquid Metal on Solid Ionocovalent Oxide Surface", *Rare Metals*, Vol 12 (2), pp 84-96.
15. Fowkes, F.M., (1964), "Attractive Forces at Interfaces", *Industrial and Engineering Chemistry*, Vol 56 (12), pp 40-52.
16. Chattoraj, D.K., Birdi, K.S., (1984), *Adsorption and the Gibbs Surface Excess*, New York: Plenum Press.
17. Good, R.J., Girifalco, L.A., (1960), "A Theory for Estimation of Surface and Interfacial Energies: Estimation of Surface Energies of Solids From Contact Angle Data", *Journal of Physical Chemistry*, Vol 64, pp 561-565.
18. Agathopoulos, S., Nikolopoulos, P., (1995), "Wettability and Interfacial Interactions in Bioceramic-Body-Liquid Systems", *Journal of Biomedical Materials Research*, Vol 29, pp 421-429.
19. Lawrence, J., (1998), "The Characteristics and Feasibility of High Power Diode Laser Ceramic Tile Grout Sealing", PhD Thesis, UMIST. *To be submitted*
20. Kokai, F., Amano, K., Ota, H., Umemura, F., (1992), "Laser Ablation of Yttria Stabilised Zirconia: Etch Depth and Characterisation of Ablated Surfaces", *Applied Physics A - Materials Science & Processing*, Vol 54 (4), pp 340-342.
21. Nicolas, G., Autric, M., Marine, W., Shafeev, G.A., (1997), "Laser Induced Surface Modifications on ZrO₂ Ceramics", *Applied Surface Science*, Vol 109/110, pp 289-292.
22. Filotti, L., Bensalem, A., Shafeev, G.A., (1997), "A Comparative Study of Partial Reduction of Ceria via Laser Ablation in Air and Soft Chemical Route", *Applied Surface Science*, Vol 110, pp 249-253.
23. Shafeev, G.A., Sissakyn, E.V., (1997), "Laser Induced Surface Modifications of LiNbO₃", *Laser Physics*, Vol 3, pp 110-120.
24. Lawrence, J., Li, L., Spencer, J.T., (1998), "Diode Laser Modification of Ceramic Material Surface Properties for Improved Wettability and Adhesion", *Applied Surface Science*, Vol 116, pp 195-201.

Mr. Jonathan Lawrence graduated from the University of Bradford in 1994 with an honours degree in Mechanical Engineering. He is currently completing the final year of a PhD project to study the feasibility of high power diode laser ceramic tile grout sealing. Dr. Lin Li is head of the Laser Laboratory and a lecturer at UMIST. Dr. Julian Spencer is a Senior Research Associate, managing laser projects at the BNFL Company Research Laboratory.